Reproductive Biology 20 (2020) 97–105

Contents lists available at ScienceDirect

Reproductive Biology

journal homepage: www.elsevier.com/locate/repbio

Chitosan coating does not prevent the effect of the transfer of green silver nanoparticles biosynthesized by *Streptomyces malachitus* into fetuses via the placenta

Khloud Elsharawy[a], Mohamed Abou-Dobara[b], Hekmat El-Gammal[a], Ayman Hyder[a,*]

[a] Departments of Zoology, Faculty of Science, Damietta University, Egypt
[b] Departments of Botany & Microbiology, Faculty of Science, Damietta University, Egypt

ARTICLE INFO

Keywords:
Green silver nanoparticles
Streptomyces malachitus
Chitosan coating
Nanotoxicology
Maternal-fetal exchange
Placental toxicity

ABSTRACT

Green synthesized nanoparticles are more advantageous over conventionally prepared ones due to less toxicity, production cost, and environmental hazards. With the widespread of the utilization of nanoparticles, little is known about the maternal-fetal transplacental transfer of green nanoparticles. We have biosynthesized silver nanoparticles using metabolites of *Streptomyces malachitus* and sunlight then coated them with chitosan. These nanoparticles have been characterized and intraperitoneally administered at doses of 100 mg/kg on the 6th, 8th, and 10th gestational days. On the 18th day of pregnancy, both coated and non-coted NPs were detected in different maternal tissues, placenta, and in fetuses, as determined by estimation of silver content and observation by electron microscopy. Chitosan coating decreased the silver content in different tissues, maybe due to the larger size of coated nanoparticles that retards the transfer. The toxic effects on maternal and fetal tissues were proportional to their silver content, as determined by the liver and kidney functional analysis of pregnant rats and the ultrastructural and histopathological examination of the maternal liver, placenta and fetal liver. The present data suggest that green silver nanoparticles biosynthesized by *Streptomyces malachitus* cross the placenta and have toxic effects on maternal tissues, placenta, and fetus. Chitosan coating of these nanoparticles decreases the transfer, and consequently, the toxicity. However, it does not prevent this toxicity.

1. Introduction

Nanotechnology is an emerging multidisciplinary field widely used in basic science, industry and medical fields. Different kinds of nanoparticles (NPs) are applied among other applications in gene delivery and silencing [1–3], drug delivery [4], and cancer therapy [5,6]. Of particular interest, silver nanoparticles (AgNPs) have been used for enormous applications including pharmaceutical and food industry, healthcare-related products, diagnostics medical device coatings, orthopaedics, biosensors and cosmetics [7]. AgNPs have been reported to possess antibacterial [8], anti-fungal [9], anti-inflammatory [10], antiviral [11] and anti-angiogenesis [12] characteristics.

Despite all of these applications, it has been reported by many *in vivo* toxicity studies that AgNPs have toxic effects on the lung, liver, brain and other cells in adult animals [13–15]. Numerous factors including size, shape, surface charge and surface coating were known to influence in AgNPs toxicity. The surface coating affects the affinity of AgNPs for the cell surface and the release of free silver ions from AgNPs, which was also proposed as a toxicity mechanism for AgNPs [16–19]. Different organic materials have been employed to modify NP properties through surface modification. of which, chitosan which is a non-toxic biopolymer with important biological [20], antimicrobial [21], hypocholesterolemic [22] and drug delivery activities [23,24].

Green biosynthesis of nanoparticles using microorganisms and plant-derived products could serve a better strategy than traditional physical and chemical synthesis of nanoparticles to achieve economic, social, health and environmental benefits [25,26] These conventional methods are expensive, energy-consuming and hazardous to the environment [27]. Previous studies suggested less toxicity of green-synthesized than chemically or physically-prepared NPs. According to previous reports, exposure to free silver ions which highly associated with AgNPs toxicity [16] may produce toxic effects which can negatively affect the liver, kidney, eye, and skin, cause respiratory problems, and lead to tract irritations of intestinal and changes in blood cells [28,29]. Green synthesized AgNPs have far less free ions than that prepared by conventional methods. In addition, green AgNPs can be

* Corresponding author at: Faculty of Science, Damietta University, New Damietta 34517, Egypt.
E-mail address: hyder@du.edu.eg (A. Hyder).

https://doi.org/10.1016/j.repbio.2020.01.004
Received 9 December 2019; Received in revised form 12 January 2020; Accepted 14 January 2020
Available online 07 February 2020
1642-431X/

preferred than chemical ones due to some chemicals in the bio-reducing agent that provide a non-toxic coating on AgNPs [30].

Recent studies have revealed that different kinds of nanoparticles are able to penetrate the placental barrier into fetal organs after administration to pregnant females [31–33]. This transfer was found to be size-dependent [34] and has many cytotoxic and genotoxic effects on mother and fetuses [35,36]. Even low doses that do not cause significant change in gene expressions in the placenta have been found to affect developing brains that showed the most sensitivity to the nanoparticle exposure [37,38]. The same is also valid for silver nanoparticles [39], which are nowadays used in plastics, cosmetics [40] and other women products. This may affect embryos/fetuses in case of pregnancy since foetuses are more sensitive to environmental toxins than adults [41]. Studies that deal with the maternal-fetal transfer of AgNPs are scarce [33, 42]. None of them studied the transfer from mother to the fetus of green biosynthesized AgNPs, which may be preferred due to less toxicity, and evaluate the toxic effect on the fetus.

In the present study, we have recruited *Streptomyces malachitus* to biosynthesize silver nanoparticles. *Streptomyces* is a safe microorganism for the production of several antibiotics and enzymes of commercial value. A previous study has used *Streptomyces hygroscopicus* for the biosynthesis of AgNPs [43]. These green-synthesized AgNPs were applied in pregnant rats to evaluate whether a placental transfer into foetuses occur and the effect of these newly prepared NPs on both mother and foetus. In one group, we have coated the AgNPs with chitosan to minimize their toxicity, if any.

2. material and methods

2.1. Microorganisms

Streptomyces malachitus used in the synthesis of AgNPs was isolated from a fertile soil sample and identified according to the International *Streptomyces* Project [44,45]. A spores' suspension of *S. malachitus* was maintained at −80 °C in a 20 % (w/v) glycerol aqueous solution in the laboratory of Microbiology, Botany and Microbiology Department, Faculty of Science, Damietta University, Egypt.

2.2. Culturing conditions and production of metabolites

The organism was grown in starch nitrate agar medium for 7 days at 30 °C; three discs (each 1 cm in diameter) of the obtained growth were inoculated into 250 ml Erlenmeyer flasks containing 50 ml of starch-nitrate broth medium [45] then incubated at 30°C for 7 days. The extracellular produced metabolites were separated by centrifugation at 5,000 rpm for 10 min.

2.3. Synthesis of silver nanoparticles

AgNPs were synthesized by treating 10 ml of 10 mM silver nitrate with 0.5 ml of *S. malachitus* metabolite. The reaction flask has been exposed to direct sunlight irradiation for 20 min. A sample left in dark served as control. Turning the color into brown was used as an indicator of the biosynthesis of AgNPs. This color is a result of excitation of surface plasmon resonance and reduction of Ag^+ ions to Ag metal by the reducing agents in metabolites [46,47]. The weight of resulting AgNPs was estimated after precipitation by centrifugation of the previously prepared reaction at 10,000 rpm for 30 min and drying at room temperature.

2.4. Preparation of chitosan coated silver nanoparticles

Chitosan solution was prepared by dissolving purified CS in 0.5 % acetic acid solutions to reach a concentration of 1 % (wt/v) under magnetic stirring for 12 h until solutions were transparent. Once dissolved, this solution was collocated with AgNPs in a proportion of 28:1. This solution was mixed for 12 h at room temperature [48].

2.5. Characterization of silver nanoparticles

2.5.1. Ultraviolet (UV)-visible spectral analysis

The biosynthesized silver nanoparticles were monitored by measuring the UV–Vis spectra of the reaction mixture (aqueous silver nitrate solution with *S. malachitus* metabolites). AgNPs were preliminarily characterized by the sample absorption spectra from 300 to 650 nm using a UV–vis spectrophotometer (Unico 7200). A sample left in dark was used as a control throughout the experiment. Also, UV–vis spectra of coated AgNPs sample dispersed in distilled water were estimated.

2.5.2. Analysis of fourier transforms infrared spectroscopy (FTIR) and zeta potential

FTIR spectra of AgNPs and CS-AgNPs have been recorded by a Thermo Nicolet Nexus 470 and Mattson 5000 FT-IR spectrometers with only selected absorptions being recorded. About 2 mg of the samples were grounded thoroughly with KBr and the pellets were prepared using a hydraulic press under a pressure of 6000 kg cm^{-2}. The nano colloidal solution stability and surface charge of AgNPs and CS-AgNPs were measured by Zeta Potential Analyzer, model Malvern Zeta-size Nano-zs90, U.S.A. Samples were diluted 1:15 with distilled water prior to measurement.

2.5.3. Transmission Electron microscope (TEM) analysis

Size and shape of AgNPs and CS-AgNPs were examined by TEM (TEM, JEOL JEM-100CX, USA) at Electron Microscope Unit, Mansoura University, Egypt.

2.6. Experimental animals

Male and female Wistar rats weighing 100–120 g were used in the present study. Rats were obtained from Helwan Company for vaccines and medicines, Cairo, Egypt. Animals were maintained in the animal house of the Zoology Department, Faculty of Science, Damietta University, with food and water *ad libitum*. They were housed in well-ventilated cages under standard environmental conditions (25 ± 2 °C, 45–55 % relative humidity, and 12 h dark/light cycle) and allowed 2 weeks for acclimatization.

2.7. Experimental design

Normally, 1:1 (one male to one female) mating was used in this study. Mating was confirmed by the presence of sperm in the vaginal smear, designated day 0 of gestation (GD0), and the pregnant dams were weighed and moved to pairwise housing with another pregnant female. Dams were assigned to 3 groups of 4 animals each, a control group, AgNPs treated group and CS-coated AgNPs group. Pregnant rats were 3 times intraperitoneally injected in GD6, GD8, and GD10 with 100 mg/kg AgNPs or CS-coated AgNPs. On day 18 of gestation, the liver, kidney, brain, placenta and the fetuses were excised and processed for different examinations.

2.8. Histopathological analysis

Samples (mothers' liver, placenta, fetus' liver) were subsequently fixed in 10 % neutral buffered formalin and processed to the conventional hematoxylin and eosin stain for microscopic examination [49].

2.9. Ultrastructural examination

The mother's liver, placenta and fetus' liver of the studied groups were dissected and fixed by immersing them immediately in in 2 % glutaraldehyde, postfixed in 1 % osmium tetroxide for 2 nh at 4 °C, infiltrated in resin. Ultrathin (50−70 nm thickness) sections were cut

using an LKB ultramicrotome (LKB Produkter AB, Ltd., Stockholm, Sweden) and stained with uranyl acetate and lead citrate [50]. The stained sections were then examined using the transmission electron microscope (JEOL JEM-100CX, USA).

2.10. Silver content analysis

Animals' liver, kidney, brain, and placenta were digested using a mixture (at a ratio of 2:1 v/v) of nitric acid (1 M) and perchloric acid (1 M) for 3 h and then incubated at 120 °C (to remove the remaining acids). Each sample was diluted with distilled water up to a known volume and used for silver (Ag) total mass measurement by flame Atomic Absorption Spectrometer (PerkinElmer, PinAAcle 500PinAAcle 500, UK).

2.11. Biochemical analyses

Blood samples were collected and serum was harvested and stored at 20 °C until the determination of alanine aminotransferases (ALT), albumin, as well as creatinine according to standard methods as previously described [51]

2.12. Statistical analysis

The data for each group were expressed as mean ± standard deviation. The independent one way ANOVA was used for data analysis followed by student's *t*-test as a posthoc test, whenever ANAVA was significant. The statistical significance of all data was set at $p < 0.05$. Microsoft Excel 2013 software was used for producing diagrams.

3. Results

3.1. Characterization of silver nanoparticles

The produced AgNPs had amorphous shapes, mostly near round, and different sizes ranging from 7 to 35 nm (ture 1A) with an average size of 19.50 ± 6.72 nm (mean ± SD).

3.1.1. FTIR analysis

Fig. 1B shows the FTIR of the AgNPs. The observation of band at 3426 cm^{-1} exemplifies the OH and NH stretching of sulfur-containing proteins and/or NADH dependent enzymes which have excellent redox properties. The absorption of the band at 1628 cm^{-1} denotes the C═O stretching of the amide group. The peak at 1384 cm^{-1} corresponding to the N═O bending of nitro groups. The bands observed at 981 cm^{-1} represent the C−O and CC−. Fig. 1C and D show the FTIR spectra of chitosan-coated AgNPs and chitosan, respectively. The bands at 3418 cm^{-1} and 3442 cm^{-1} were related to the stretching vibrations of amino groups from NH-amine. The bands less than 2990 cm^{-1} corresponded to the alkane C−Hs−tretching lipids. The bands between 1650 cm^{-1} and 1550 cm^{-1} corresponded to the amino groups of amide. The bands between 1330 cm^{-1} and 1400 cm^{-1} were associated with the C═C stretching of aromatic amine groups. The bands between 1080 cm^{-1} and 1030 cm^{-1} were related to the carbonyl stretch in proteins.

3.1.2. Zeta potential

Analysis of Zeta potential of biosynthesized AgNPs showed a sharp peak at −19.6 mV that indicated the biogenic nanoparticles were negatively charged on their surfaces as shown in Fig. 1E. While the surface charge of chitosan-coated AgNPs was positive and zeta potential was 11.9 (Fig. 1F). It can be assumed that chitosan components, due to their high affinity to bind to AgNPs surface attaching thiols and amino groups might be modifying electrical charges on the surface of AgNPs producing differences on the surface charge of the outer region of AgNPs [52].

3.1.3. UV–vis spectrophotometer

The observation of color change is an analysis to identify the synthesis of silver nanoparticles using *S. malachitus* extract. Fig. 1G exhibits the UV–Vis spectrum of silver nanoparticles synthesized by using *S. malachitus* which exhibited a strong absorption band at 441 nm. However, the presence of biomolecules on coated AgNPs promoted larger bands from 600–800 nm as shown in Fig. 1H.

3.1.4. Ultrastructural analysis

TEM micrographs of AgNPs and chitosan-coated silver NPs are shown in Fig. 1I–K. The biosynthesized AgNPs were spherical and well disperse (Fig. 1I). Chitosan-coated AgNPs samples (Fig. 1J) show uniform spherical shapes while bigger nanoparticles are pseudospherical particles with irregular hexagonal shapes. Coated AgNPs exhibit acceptable dispersion and good size distribution. A small shell coated AgNPs sample (around the 4 nm) was also observed around the pseudospherical AgNPs (Fig. 1K).

3.2. Chitosan coating partially protects rat dams against the effect of AgNPs

Pregnant rats were injected on the gestational days 6, 8 and 10 with either coated or non-coated green silver NPs. The determination of NP penetration in dams and pups depended on NP observation by electron microscope examination and the estimation of tissue content of silver. The effects of these green NPs were assessed by examination of liver and kidney functions and histopathological examination.

3.2.1. Silver content in tissues

We have tested the penetration of Ag-NPs into the mother rats. The liver, kidney, brain, and placenta in these rats have been analyzed for their content of silver. The results revealed a significant increase in silver content in both groups in the liver, kidney, and brain (ANOVA $p < 0.02$, $p < 0.000001$, $p < 0.0003$, respectively, Fig. 2A). However, the silver concentration in the liver and kidney of rats injected with coated NPs was significantly lower than in those injected with non-coated NPs (*t*-test, $p < 0.05$).

3.2.2. Ultrastructure of the maternal liver

The ultrastructural examination of maternal liver parenchymal cells showed degenerating hepatocytes of the AgNPs group. Cells had small nuclei with clumped chromatin and many sites of disruptions in the nuclear membrane. The cytoplasm revealed numerous lesions of subcellular organelles and many deposits of AgNPs. The degenerated mitochondria had fewer cristae than normal, and some had internal inclusions including deposits of silver nanoparticles. Many secondary lysosomes with heterogeneous electron densities were observed. The cytoplasm had wide irregular areas filled with ribosomes. Rough endoplasmic reticulum had dilated cisternae, while smooth endoplasmic reticulum was vesiculated (ex. Fig. 2B). In the chitosan-coated AgNPs group, the transmission electron microscopic examination showed that liver parenchymal cells kept most of their normal ultrastructural architecture, although fewer deposits of silver nanoparticles have been observed. However, quantitative analysis of NP deposits was not possible. Hepatocytes showed large euchromatic nuclei and prominent nucleolus. Normal mitochondrial cristae, rough endoplasmic reticulum with ribosomes and secondary lysosomes with heterogeneous electron densities have been observed.

3.2.3. Biochemical analysis

The maternal liver function was tested by measuring ALT (Fig. 2C) and albumin (Fig. 2D) after treatment with either chitosan-coated or non-coated AgNPs. The results revealed significant increases in the hepatic enzyme ALT as well as albumin after treatment with naked NPs. However, no statistical difference was observed in the hepatic function of coated-NPs-treated female rats. These parameters have not been changed and were significantly lower in rats treated with coated than in

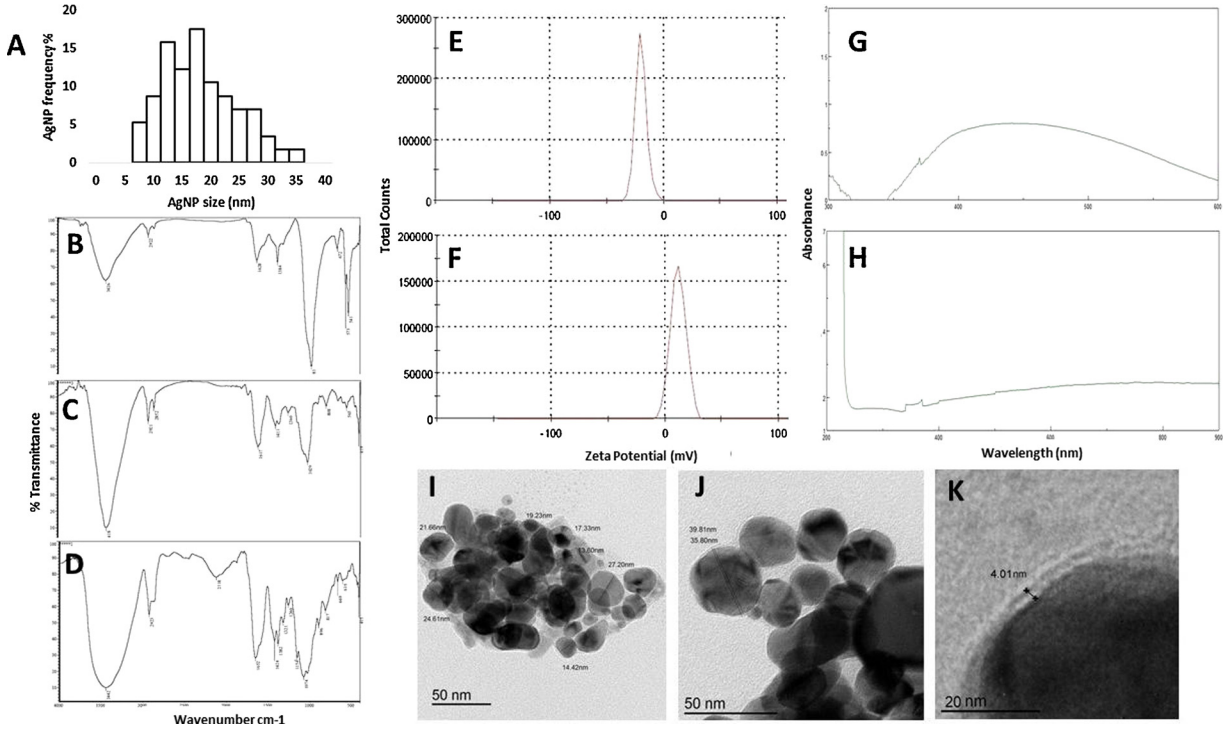

Fig. 1. Characterization of silver nanoparticles biosynthesized by *Streptomyces malachitus* and coated by chitosan. (A) size and frequencies of the produced AgNPs. B–D are the FTIR analysis for AgNPs (B), chitosan-coated AgNPs (C), and chitosan only (D). Zeta potential of AgNPs showed a sharp peak at −19.6 mV (E), while the surface charge of chitosan-coated AgNPs was positive and zeta potential peaked at 11.9 (F). The UV–Vis spectrum of AgNPs exhibited absorption band at 441 nm (G), while coated AgNPs showed larger bands at 600–800 nm (H). I–K represent the electron microscopic figures of AgNPs (I), chitosan-coated AgNPs (J), and the magnified chitosan coat around a NP (K).

that treated with non-coated NPs.

Similarly, kidney function was assessed by measuring blood creatinine in all groups (Fig. 2E). Silver nanoparticles caused a significant increase in creatinine, while chitosan coating prevented significantly this increase.

3.2.4. Histopathological investigation of the maternal liver

Histologic examination of control maternal liver parenchyma (Fig. 2F) revealed hepatic lobules formed of cords of hepatocytes radiating out from the terminal hepatic venule. These cell cords were separated by narrow hepatic sinusoids lined with specialized fenestrated endothelial cells and macrophages (Kupffer cells). Each lobule was surrounded by a portal area of scanty connective tissue containing branches of the hepatic portal vein, hepatic artery, and bile ductile.

Histologic examination of liver from pregnant rats that received AgNPs (Fig. 2G) exhibited histopathological lesions in comparison to the control group. Disarrangement of hepatic tissue architecture; necrotic hepatocytes; prominent ballooning degeneration as hepatocytes became swollen, rounded, and pale stained, congested and dilated portal vein with thickened wall and leukocyte infiltrations in the portal area have been observed.

In the chitosan-coated-AgNPs group (Fig. 2H), maternal liver sections revealed fewer histopathological lesions in comparison to that found in the non-coated group. The hepatic lobules showed maintained architecture with a normal organization. Most hepatocytes showed normal appearance, although some degenerated and necrotic hepatocytes as well as periportal infiltration, dilated portal vein with thickened wall can still be recognized.

3.3. Both non-coated and chitosan-coated silver nanoparticles pass to the placenta

We have analyzed the placental content of silver after both treatments (Fig. 3A), and found a significantly high silver concentration in both treated groups than that in the control group (ANOVA $p < 0.0001$, *t*-test $p < 0.0001$ for both groups, compared with the control). However, this silver concentration was significantly lower in coated NP group than in the non-coated one ($p < 0.03$)

3.3.1. Ultrastructure of placenta

Transmission electron microscopic examination of the maternal-fetal barrier in the labyrinthine zone of the placenta in the AgNPs treated group demonstrated many deposits of AgNPs within the cytoplasm of cytotrophoblast and syncytiotrophoblast (Fig. 3B, C). The sloughed cytotrophoblast revealed apoptotic nuclei with clumped chromatin and undulations of the nuclear membrane, mitochondrial injury and degeneration, intracytoplasmic vacuolization, and degeneration of both smooth and rough endoplasmic reticulum. The peripheral chromatin condensation in the fetal capillary endothelial cell nucleus and undulations in the boundaries of the nucleus were seen. Disorganization of the cytoplasmic structure, debris of degenerated organoids and an increase in the number of vesicle-like structures in the cytoplasm of syncytiotrophoblast were detected.

3.3.2. Histopathological examination of placenta

Histological sections of the control rat placenta showed normal maternal and fetal architectures (Fig. 3D, E). The fetal part consisted of two distinct zones; essentially the labyrinth zone and the basal zone. The labyrinth zone, which is the most extensive part of the placenta, was formed of maternal sinusoids and fetal capillaries separated from each other by the placental barrier. The barrier was composed of the following layers in succession; the endothelium and basement membrane of the fetal blood capillary, fetal mesenchymal tissue, syncytiotrophoblast, and cytotrophoblast. The syncytiotrophoblast was made up of syncytial elongated multinucleated cytoplasm with ill-defined cell boundaries. The cytotrophoblast consisted of low cuboidal cells with

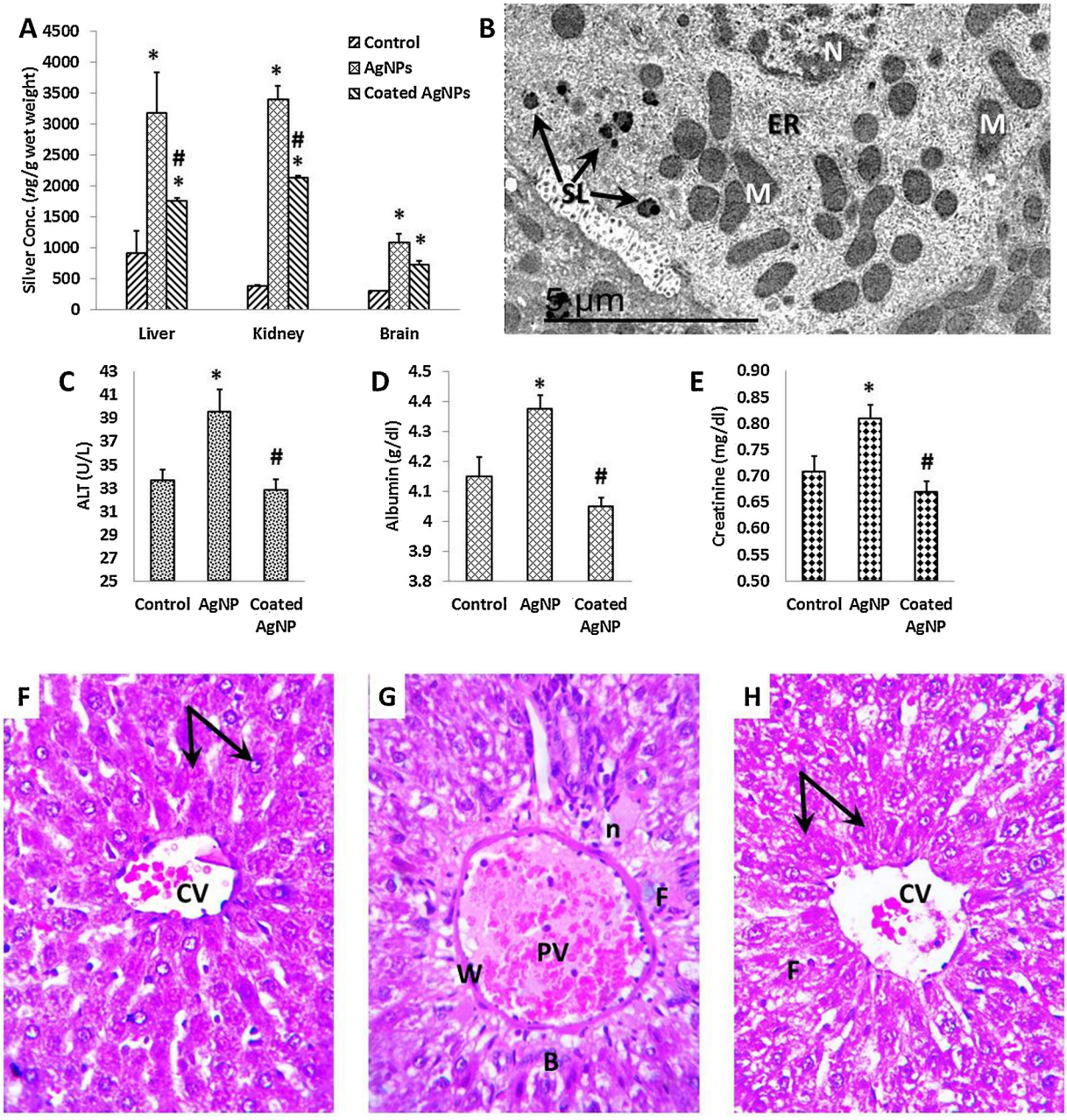

Fig. 2. Effect of silver nanoparticles biosynthesized by *Streptomyces malachitus* on pregnant rats. Female rats administered ip doses of 100 mg/kg AgNPs or coated AgNPs on the 6th, 8th and 10th gestetional days and tissues were harvested on the 18th gestetional day. (A) Silver content in different tisses of female rats, (B) TEM of of liver of AgNP-receiving rats shown mitochondria (M); endoplasmic reticulum (ER); secondary lysosomes containing NPs (SL), and nucleus (N). Livr and kidney functions were assessed by estimating serum alanine aminotransferase (ALT) (C), albumin (D) and creatinine (E) in different groups. Histological analyses of control, AgNP group and coated-AgNP group are represented in photomicrographs F, G,and H, respectively, and showing central hepatic vein (CV); portal vein (PV); necrotic hepatocyte (n); thickened wall of portal vein (W); ballooning hepatocyte (B); periportal infiltration (F), and cords of hepatocytes (arrows). When applicable, data are presented as mean ± SEM of N = 4. Statistical analyses: difference between groups was significant for all applicable parameters (ANOVA). * denotes significantly different value from the control one; # denotes significantly different value from the value of the non-coated AgNP group (student's *t*-test after ANOVA significance).

microvillous surface and large spherical nuclei. The basal zone demonstrated three types of differentiated cells; spongiotrophoblasts, trophoblastic giant cells and clusters of glycogen containing cells, all present in between maternal sinusoids. The spongiotrophoblasts cells constituted the majority of the cells in the basal zone. The spongiotrophoblasts were small rounded cells with oval or rounded central nuclei. Trophoblastic giant cells were mainly located at the maternofetal interface. They varied in size and shape with two or more nuclei. The cytoplasm of the cells exhibited deep basophilia. Glycogen containing cells showed multiple small cell masses and islands. They were seen principally in the basal zone.

Placenta of AgNPs treated rats (Fig. 3F, G) showed definite lesions in comparison to the control group. The labyrinth zone showed markedly dilated and congested fetal capillaries, decreased number of trophoblasts, and a reduction in thickness of trophoblastic trabecula and irregular dilatation of maternal sinusoids. Cytotrophoblastic cells showed sloughing, vacuolated cytoplasm and necrotic nuclei. The syncytiotrophoblastic cells revealed sloughing and apoptosis. Apparently there is an increase in mesenchymal tissue and trophoblastic cells that surround the fetal capillaries. The placental basal zone of AgNPs treated

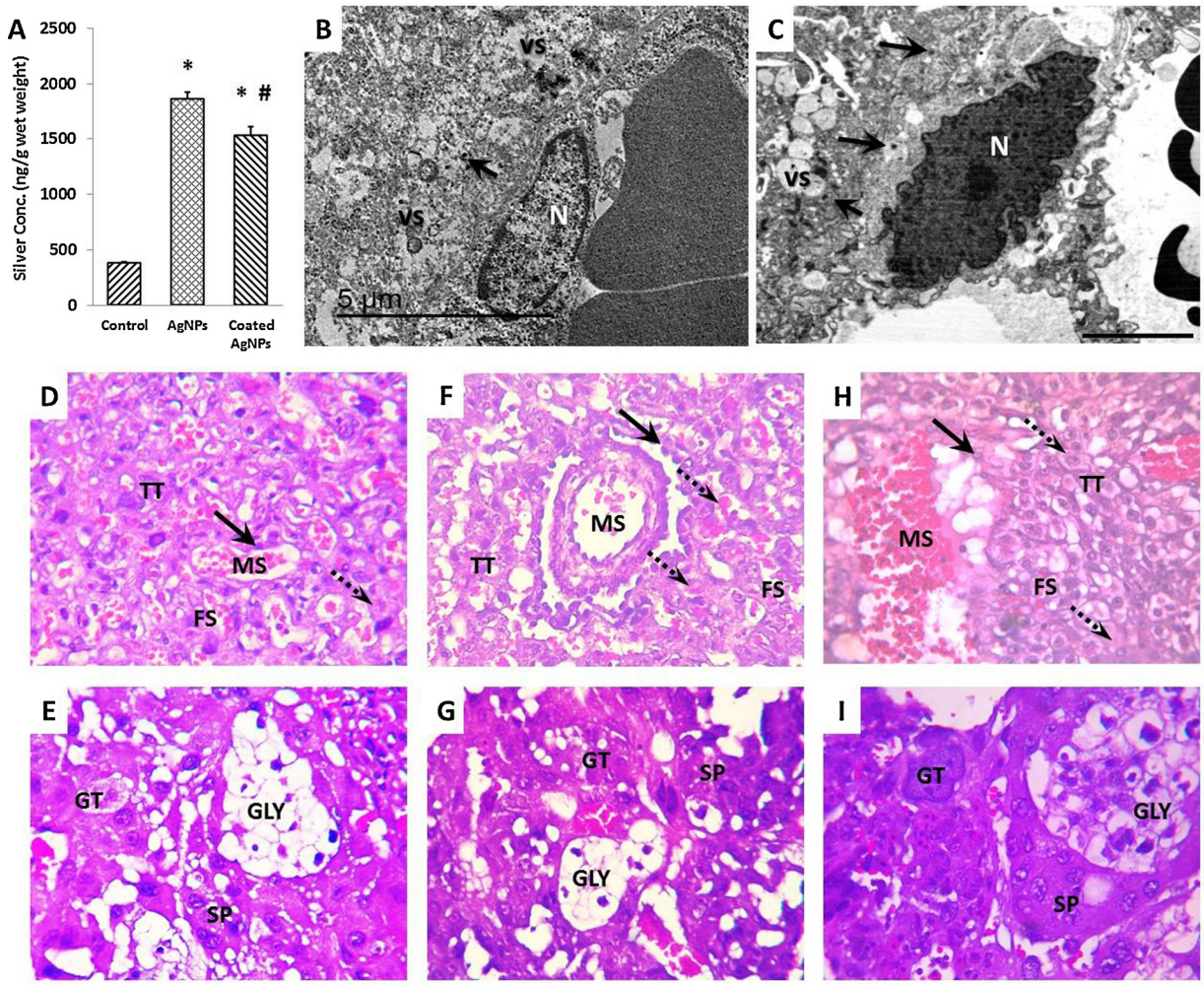

Fig. 3. Silver nanoparticles biosynthesized by *Streptomyces malachitus* are detected in rat placenta. Placenta was excesed on the 18th gestetional day from pregnant rats administered ip doses of 100 mg/kg AgNPs or coated AgNPs on the 6th, 8th and 10th gestetional days. (A) silver content in the placenta of different groups. Data are presented as mean ± SEM of N = 4. The difference between groups was statistically significant (ANOVA). * denotes significantly different value from the control one; # denotes significantly different value from the value of the non-coated AgNP group (student's *t*-test). B and C: TEM of pacenta frem AgNP and coated- AgNP, respectively, and showing nucleus (N); deposits of Ag-nanoparticles (arrows) and vesicle-like structures (VS). D–I: photomicrographs of placentae from control (D, E), AgNP (F, G), and coated-AgNP (H, I) groups showing maternal sinusoids (MS); fetal capillaries (FS); trophoblastic trabecula (TT); cytotrophoblast (arrows); syncytiotrophoblast (dotted arrows); giant trophoblastic (GT); spongiotrophoblasts (SP) and Glycogen cell (GLY).

rats showed marked histopathological lesions. These lesions represented by hypoplasia of spongiotrophoblasts, cytolysis of glycogen cells, fibrinoid necrosis and cystic dilation.

Treatment with chitosan-coated AgNPs (Fig. 3H, I) greatly decreased the placental tissue lesions induced by AgNPs. Placental labyrinth zone from the coated NP-treated group showed an increased number of trophoblasts, amelioration in the thickness of trophoblastic trabecula, decreased mesenchymal tissue, and decreased number of sloughed trophoblastic cells. Congestion of placental vasculature were seen. The placental basal zone of chitosan-coated-AgNPs-treated rats revealed a marked decrease in histopathological lesions in comparison to AgNPs treated group. Signs of this improvement were the increased number of spongiotrophoblasts, normal structure of glycogen cells, absence of fibrinoid necrosis, and cystic dilation.

3.4. Histopathological examination of the fetal liver

Histological examination of fetal liver on gestational day 18 from the control mother (Fig. 4D) showed a normal fetal hepatic architectural appearance. The normal hepatic tissue illustrated central vein within loosely, haphazardly arranged hepatic cords that are several hepatocytes thick and contain abundant intrahepatocellular glycogen. The primitive sinusoids that separated disorganized cords of hepatocytes and scattered megakaryocytes were seen. Extramedullary hematopoiesis was observed and composed of islands of erythropoiesis within the sinusoids. The portal tract from the control fetal liver contains a portal vein surrounded by immature biliary structures. Some of the biliary structures were of the two-cell thick ductal plate configuration. Extramedullary hematopoiesis was observed and composed of islands of erythropoiesis within the sinusoids, scattered megakaryocytes, and myelopoiesis surrounding the portal vein. The mesenchyme (connective tissue) at the portal area was absent.

The liver of fetuses on gestational day 18 maternally treated with AgNPs (Fig. 4E) displayed hepatic lesions associated with degeneration and necrosis of hepatocytes, vacuolization and sloughing of cells within the central vein, and some intrahepatocellular glycogen. Extramedullary hematopoiesis was decreased and composed of few islands of erythropoiesis within the primitive sinusoids. The hepatic portal tract of fetuses maternally treated with AgNPs exhibited degeneration and necrosis of hepatocytes, vacuolization, congestion of hepatic vein, and degeneration of ductal cells in the immature biliary structures. A reduction in extramedullary hematopoiesis was seen.

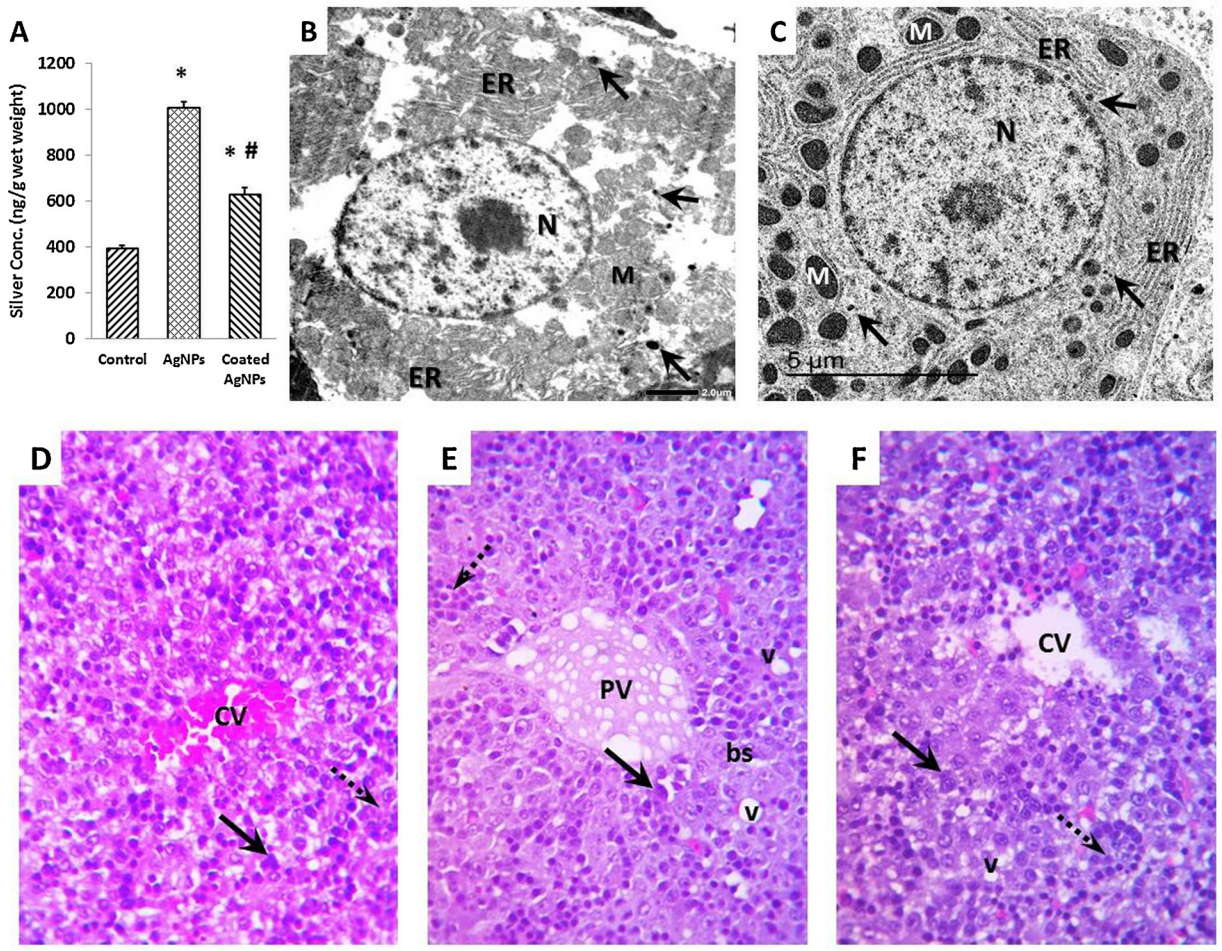

Fig. 4. green silver nanoparticles passes through the pacenta to the fetus. Fetuses were harvested on the 18th gestetional day from rats received ip doses of 100 mg/kg AgNPs or coated AgNPs on the 6th, 8th and 10th gestetional days. (A) silver content in fetuses of different groups. Data are presented as mean ± SEM of N = 4. The difference between groups was statistically significant (ANOVA). * denotes significantly different value from the control one; # denotes significantly different value from the value of the non-coated AgNP group (student's *t*-test). B and C: TEM of fetal liver frem AgNP and coated- AgNP, respectively shown nucleus (N); deposits of Ag-nanoparticles (arrows); mitochondria (M); endoplasmic reticulum (ER); D–F: photomicrographs of fetal liver from control (D), AgNP (E), and coated-AgNP (F) groups showing islands of erythropoiesis (dotted arrows); megakaryocytes (arrows); vacuolization (V) and central vein (CV).

In the coated AgNP group, fetal liver (Fig. 4F) revealed mild hepatic lesions represented by cells sloughing within the central vein and some vacuolization. Improvement in intrahepatocellular glycogen and extramedullary hematopoiesis were seen. The hepatic portal tract of fetuses on gestational day 18 maternally treated with coated AgNPs tend to be similar to normal architecture. The hepatic portal tracts were generally normal in appearance and structure although some vacuolization and hyalinization of the hepatic vein can be seen.

4. Discussion

The green synthesis of nanomaterials has many advantages over conventional chemical and physical synthesis methods as lowering production cost, avoiding environmental pollution, reducing physiological toxicity, and enhancing biological compatibility [53]. The achievement of greener design for the synthesis of nanoparticles depends on the selection of environmentally benign chemicals and on the methodological considerations. Cinelli et al. [54] have developed an evaluation model to assess the synthesis protocols of nanoparticles. The selected criteria used in that model included a reducing agent, a capping agent, solvent typology, use of local resources, reaction time, reaction temperature, equipment type, and size range of ensuing nanoparticles. Based on these criteria, the biosynthetic method developed in this study for producing AgNPs has distinct advantages over most other known methods. Since the metabolite of *S. malachitus*, including pigment; represents the bio-reductant medium (reducing agent, capping agent, and solvent). This is renewable, easy to be prepared at low cost and used in small amounts. Also, one main drawback of biosynthesis of AgNPs is the long reaction time [55]. The present protocol is performed within minutes at room temperature in the presence of sunlight. This guarantees high biosafety, low cost, less consumption of energy, speed and simplicity of operation.

The characterization of these biosynthesized AgNPs in the present study revealed similarity with previously described AgNPs. In the UV–vis spectrum, a strong and broad peak was observed between 420 − 450 nm indicating the presence of AgNPs. These results are in concordance with other studies synthesized AgNPs by other biological sources such as *Streptomyces hygroscopicus* [43], *Penicillium chrysogenum* cell filtrate [56], *Taraxacum officinale* leaf extract [57] and dried *Ficus benghalensis* root extract [58]. Larger bands obtained from coated AgNPs indicated the presence of chitosan on the surface of nanoparticles, and this result is comparable to that of another study [48]. FTIR spectra confirmed the presence of proteins that could be playing a significant role in the synthesis of AgNPs and their stability. Sulfur-containing proteins and/or NADH dependent enzymes that have excellent redox properties. The reducing agents are the major compounds present in the *S. malachitus* metabolite might be acting as cofactors in the reduction of silver ions and the subsequent formation of AgNPs

[59]. The silver nanoparticles were bonded by proteins, which served as a stabilizing agent, either through free amine groups or cysteine residues [60]. The comparison of the FTIR spectra of chitosan-coated AgNPs with those of AgNPs and chitosan gives an elementary idea of the presence of both of the constituents in the self-assembled polymer-coated AgNPs. Zeta potential analysis indicated that the biogenic nanoparticles are negatively charged on their surface [61] while the chitosan-coated AgNPs positively charged due to the high affinity of ionic silver to attach to free amino groups of chitosan.

Many studies have demonstrated that the exposure of silver nanoparticles led to silver accumulation in various organs including liver, kidneys, testes, lungs, and brain [62–64]. In fact, we have similar results. As the liver is able to actively remove compounds from the blood and transform those to chemical forms that can easily be excreted by the kidney, we, therefore, focused on liver and kidney function to compare the toxicity of chitosan-coated and non-coated AgNPs. Significant elevations of ALT, Albumin and creatinine were observed, indicating damaging changes in liver and kidney function. Previous studies have shown that metal nanoparticles alter the levels of various biochemical markers, suggesting hepatocellular injury, hepatic inflammation, and impairment of kidney function [65]. The hepatocytic inflammation in the liver tissue of the current study is consistent with another study [66] on rat liver following nanosilver administration. Hepatocytes exhibited mild infiltration of inflammatory cells in the portal vein area.

The present data confirm that AgNPs are able to cross the placenta [67]. The four placental layers: the maternal decidua, trophoblast cell, spongiotrophoblast, and labyrinth were found to be affected by nanoparticles, with necrotic and apoptotic cells of cytotrophoblastic and syncytiotrophoblastic cells. This led to hypocellularity of trophoblasts, and consequently poor development of the placenta. It is known that poor placental development is associated with miscarriage and fetal growth restriction [42]. Normal placental development is essential for healthy embryonic development. The observed fetal deaths and resorption in the AgNPs group (data not shown) can be attributed to the effect of these AgNPs, which caused placental hypoplasia and the inability of maternal-fetal exchanges.

A number of previous studies have demonstrated that AgNPs lead to reproductive failure, embryonic death, and developmental malformations in a number of non-mammalian animal models [68,69]. Our results show that also green biosynthesized AgNPs maternally administrated during pregnancy penetrate into the fetus across placenta and lead to fetal toxicity. It should be mentioned that other routes of NPs administration such as maternal inhalation have been reported [70] to cause fetal toxicity. In the present study, fetal cyto- and histotoxicity have been proven by ultrastructural and histopathological examinations. Nonetheless, one important outcome of the present study is that the toxicity of our chitosan-coated AgNPs was minimal in fetuses. In addition to the less penetration of the larger-sized chitosan-coated nanoparticles, this toxicity has been reported to be due to oxidative stress [71]. Therefore, we suggested the minimal toxic effect observed in this study by the chitosan-coated NPs to be attributed – at least in part – to stress, which can possibly be chemically avoided by some antioxidant molecules such as N-acetyl cysteine and ascorbic acid [71]. However, this suggestion remains to be investigated.

In conclusion, these green silver NPs can be used as a drug delivery tool to target fetuses in the womb. The chitosan coat can be loaded with any drug of interest in soluble form or as a suspension. In fact, these nanoparticles are cost-effective, easy to be synthesized, easy to coat and easy to be delivered to the fetus by a single maternal injection.

Declaration of Competing Interest

None.

Acknowledgement

The work contains a part of the first author's thesis. The authors are grateful to the Faculty of Science, Damietta University, for the support and laboratory facilities. We thank Dr. Noha Omar and Dr. Ahmad Sheta from Botany and Chemistry departments, Faculty of Science Damietta University for the valuable advice and assistance during the preparation and characterization of the nanoparticles.

Appendix A. Supplementary data

Supplementary material related to this article can be found, in the online version, at doi:https://doi.org/10.1016/j.repbio.2020.01.004.

References

[1] Yang PT, Hoang L, Jia WW, Skarsgard ED. In utero gene delivery using Chitosan-DNA nanoparticles in mice. J Surg Res 2011;171:691–9.
[2] Xu Q, Zhang T, Wang Q, Jiang X, Li A, Li Y, et al. Uniformly sized iron oxide nanoparticles for efficient gene delivery to mesenchymal stem cells. Int J Pharm 2018;552:443–52.
[3] Yu Q, Qiu Y, Wang X, Tang J, Liu Y, Mei L, et al. Efficient siRNA transfer to knockdown a placenta specific lncRNA using RGD-modified nano-liposome: a new preeclampsia-like mouse model. Int J Pharm 2018;546:115–24.
[4] Kou L, Sun R, Ganapathy V, Yao Q, Chen R. Recent advances in drug delivery via the organic cation/carnitine transporter 2 (OCTN2/SLC22A5). Expert Opin Ther Targets 2018;22:715–26.
[5] Benguigui M, Weitz IS, Timaner M, Kan T, Shechter D, Perlman O, et al. Copper oxide nanoparticles inhibit pancreatic tumor growth primarily by targeting tumor initiating cells. Sci Rep 2019;9:12613.
[6] Niza E, Nieto-Jiménez C, Noblejas-López MDM, Bravo I, Castro-Osma JA, Cruz-Martínez F, et al. Poly(Cyclohexene phthalate) nanoparticles for controlled dasatinib delivery in breast cancer therapy. Nanomaterials (Basel) 2019;9(9):E1208.
[7] Zargar M, Shameli K, Najafi GR, Farahani F. Plant mediated green biosynthesis of silver nanoparticles using Vitex negundo L. extract. J Ind Eng Chem 2014;20:4169–75.
[8] Chernousova S, Epple M. Silver as antibacterial agent: ion, nanoparticle, and metal. Angew Chemie Int Ed 2013;52:1636–53.
[9] Panáček A, Kolář M, Večeřová R, Prucek R, Soukupová J, Kryštof V, et al. Antifungal activity of silver nanoparticles against Candida spp. Biomaterials 2009;30:6333–40.
[10] Nadworny PL, Wang J, Tredget EE, Burrell RE. Anti-inflammatory activity of nanocrystalline silver in a porcine contact dermatitis model. Nanomed Nanotechnol Biol Med 2008;4:241–51.
[11] Rogers JV, Parkinson CV, Choi YW, Speshock JL, Hussain SM. A preliminary assessment of silver nanoparticle inhibition of monkeypox virus plaque formation. Nanoscale Res Lett 2008;3(129).
[12] Gurunathan S, Lee K-J, Kalishwaralal K, Sheikpranbabu S, Vaidyanathan R, Eom SH. Antiangiogenic properties of silver nanoparticles. Biomaterials 2009;30:6341–50.
[13] Hyun JS, Lee BS, Ryu HY, Sung JH, Chung KH, Yu IJ. Effects of repeated silver nanoparticles exposure on the histological structure and mucins of nasal respiratory mucosa in rats. Toxicol Lett 2008;182:24–8.
[14] Sung JH, Ji JH, Yoon JU, Kim DS, Song MY, Jeong J, et al. Lung function changes in Sprague-Dawley rats after prolonged inhalation exposure to silver nanoparticles. Inhal Toxicol 2008;20:567–74.
[15] Rahman MF, Wang J, Patterson TA, Saini UT, Robinson BL, Newport GD, et al. Expression of genes related to oxidative stress in the mouse brain after exposure to silver-25 nanoparticles. Toxicol Lett 2009;187:15–21.
[16] Beer C, Foldbjerg R, Hayashi Y, Sutherland DS, Autrup H. Toxicity of silver nanoparticles - nanoparticle or silver ion? Toxicol Lett 2012;208:286–92.
[17] Suresh AK, Pelletier DA, Wang W, Morrell-Falvey JL, Gu B, Doktycz MJ. Cytotoxicity induced by engineered silver nanocrystallites is dependent on surface coatings and cell types. Langmuir 2012;28:2727–35.
[18] Kim TH, Kim M, Park HS, Shin US, Gong MS, Kim HW. Size-dependent cellular toxicity of silver nanoparticles. J Biomed Mater Res A 2012;100:1033–43.
[19] Yang X, Gondikas AP, Marinakos SM, Auffan M, Liu J, Hsu-Kim H, et al. Mechanism of silver nanoparticle toxicity is dependent on dissolved silver and surface coating in Caenorhabditis elegans. Environ Sci Technol 2012;46:1119–27.
[20] Xia W, Liu P, Zhang J, Chen J. Biological activities of chitosan and chitooligosaccharides. Food Hydrocoll 2011;25:170–9.
[21] Ahmad AL, Sumathi S, Hameed BH. Adsorption of residue oil from palm oil mill effluent using powder and flake chitosan: equilibrium and kinetic studies. Water Res 2005;39:2483–94.
[22] Zhou K, Xia W, Zhang C, Yu L. In vitro binding of bile acids and triglycerides by selected chitosan preparations and their physico-chemical properties. Lwt - Food Sci Technol 2006;39:1087–92.
[23] Park JH, Saravanakumar G, Kim K, Kwon IC. Targeted delivery of low molecular drugs using chitosan and its derivatives. Adv Drug Deliv Rev 2010;62:28–41.
[24] Liao F-H, Shieh M-J, Chang N-C, Chien Y-W. Chitosan supplementation lowers serum lipids and maintains normal calcium, magnesium, and iron status in hyperlipidemic patients. Nutr Res 2007;27:146–51.

[25] Mohanpuria P, Rana NK, Yadav SK. Biosynthesis of nanoparticles: technological concepts and future applications. J Nanoparticle Res 2008;10:507–17.
[26] Bhattacharya D, Gupta RK. Nanotechnology and potential of microorganisms. Crit Rev Biotechnol 2005;25:199–204.
[27] Liu J, Qiao SZ, Hu QH, Lu GQ. Magnetic nanocomposites with mesoporous structures: synthesis and applications. Small 2011;7:425–43.
[28] Liu W, Wu Y, Wang C, Li HC, Wang T, Liao CY, et al. Impact of silver nanoparticles on human cells: effect of particle size. Nanotoxicology 2010;4:319–30.
[29] Recordati C, De Maglie M, Bianchessi S, Argentiere S, Cella C, Mattiello S, et al. Tissue distribution and acute toxicity of silver after single intravenous administration in mice: nano-specific and size-dependent effects. Part Fibre Toxicol 2016;13(12).
[30] Allen HJ, Impellitteri CA, Macke DA, Heckman JL, Poynton HC, Lazorchak JM, et al. Effects from filtration, capping agents, and presence/absence of food on the toxicity of silver nanoparticles to Daphnia magna. Environ Toxicol Chem 2010;29:2742–50.
[31] Melnik EA, Buzulukov YP, Demin VF, Demin VA, Gmoshinski IV, Tyshko NV, et al. Transfer of silver nanoparticles through the placenta and breast milk during in vivo experiments on Rats. Acta Naturae 2013;5:107–15.
[32] Kulvietis V, Zalgeviciene V, Didziapetriene J, Rotomskis R. Transport of nanoparticles through the placental barrier. Tohoku J Exp Med 2011;225. 225–3.4.
[33] Lee Y, Choi J, Kim P, Choi K, Kim S, Shon W, et al. A transfer of silver nanoparticles from pregnant rat to offspring. Toxicol Res 2012;28:139–41.
[34] Teng C, Jia J, Wang Z, Sharma VK, Yan B. Size-dependent maternal-fetal transfer and fetal developmental toxicity of ZnO nanoparticles after oral exposures in pregnant mice. Ecotoxicol Environ Saf 2019;182:109439.
[35] Zhang Y, Wu J, Feng X, Wang R, Chen A, Shao L. Current understanding of the toxicological risk posed to the fetus following maternal exposure to nanoparticles. Expert Opin Drug Metab Toxicol 2017;13:1251–63.
[36] Pinto SR, Helal-Neto E, Paumgartten F, Felzenswalb I, Araujo-Lima CF, Martinez-Manez R, et al. Cytotoxicity, genotoxicity, transplacental transfer and tissue disposition in pregnant rats mediated by nanoparticles: the case of magnetic core mesoporous silica nanoparticles. Artif Cells Nanomed Biotechnol 2018;46:527–38.
[37] Onoda A, Umezawa M, Takeda K, Ihara T, Sugamata M. Effects of maternal exposure to ultrafine carbon black on brain perivascular macrophages and surrounding astrocytes in offspring mice. PLoS One 2014;10(9(4)):e94336.
[38] Onoda A, Takeda K, Umezawa M. Dose-dependent induction of astrocyte activation and reactive astrogliosis in mouse brain following maternal exposure to carbon black nanoparticle. Part Fibre Toxicol 2017;14(1):4.
[39] Ema M, Okuda H, Gamo M, Honda K. A review of reproductive and developmental toxicity of silver nanoparticles in laboratory animals. Reprod Toxicol 2017;67:149–64.
[40] Goswami L, Kim K-H, Deep A, Das P, Bhattacharya SS, Kumar S, et al. Engineered nano particles: nature, behavior, and effect on the environment. J Environ Manage 2017;196(297):315.
[41] Wigle DT, Arbuckle TE, Turner MC, Berube A, Yang Q, Liu S, et al. Epidemiologic evidence of relationships between reproductive and child health outcomes and environmental chemical contaminants. J Toxicol Environ Health B Crit Rev 2008;11:373–517.
[42] Kibschull M, Gellhaus A, Winterhager E. Analogous and unique functions of connexins in mouse and human placental development. Placenta 2008;29:848–54.
[43] Sadhasivam S, Shanmugam P, Yun K. Biosynthesis of silver nanoparticles by Streptomyces hygroscopicus and antimicrobial activity against medically important pathogenic microorganisms. Colloids Surf B Biointerfaces 2010;81:358–62.
[44] Shirling E, Gottlieb D. Cooperative description of type cultures of Streptomyces. IV. Species descriptions from the second, third and fourth studies. Int J Syst Evol Microbiol 1969;19:391–512.
[45] Kämpfer P, Glaeser SP, Parkes L, Keulen G, Dyson P. The family streptomycetaceae. In: DeLong EF, Lory S, Stackebrandt E, Thompson F, editors. The prokaryote: actinobacteria. 4th edNew York: Springer; 2014. p. 889–1011.
[46] Mulvaney P. Surface plasmon spectroscopy of nanosized metal particles. Langmuir 1996;12:788–800.
[47] Song JY, Kim BS. Biological synthesis of bimetallic Au/Ag nanoparticles using Persimmon (Diopyros kaki) leaf extract. Korean J Chem Eng 2008;25:808–11.
[48] Espinosa-Cristbal L, Castañón G, Loyola-Rodríguez J, et al. Bovine serum albumin and chitosan coated silver nanoparticles and its antimicrobial activity against oral and nonoral Bacteria. J Nanomater 2015;2015:9.
[49] Schrezenmeir J, Hyder A, Vreden M, Laue C, Mueller-Klieser W. Oxygen profile of microencapsulated islets: effect of immobilised hemoglobin in the alginate matrix. Transplant Proc 2001;33:3511–6.
[50] Sato S, Adachi A, Sasaki Y, Ghazizadeh M. Oolong tea extract as a substitute for uranyl acetate in staining of ultrathin sections. J Microsc 2008;229:17–20.
[51] Reitman S, Frankel S. A colorimetric method for the determination of serum glutamic oxalacetic and glutamic pyruvic transaminases. Am J Clin Pathol 1957;28:56–63.
[52] Gebregeorgis A, Bhan C, Wilson O, Raghavan D. Characterization of Silver/Bovine Serum Albumin (Ag/BSA) nanoparticles structure: morphological, compositional, and interaction studies. J Colloid Interface Sci 2013;389:31–41.
[53] Duan H, Wang D, Li Y. Green chemistry for nanoparticle synthesis. Chem Soc Rev 2015;44:5778–92.
[54] Cinelli M, Coles SR, Nadagouda MN, Błaszczyński J, Słowiński R, Varma RS, et al. A green chemistry-based classification model for the synthesis of silver nanoparticles. Green Chem 2015;17:2825–39.
[55] Liao C, Li Y, Tjong SC. Bactericidal and cytotoxic properties of silver nanoparticles. Int J Mol Sci 2019;20(449).
[56] Khalil NM, Abd El-Ghany MN, Rodríguez-Couto S. Antifungal and anti-mycotoxin efficacy of biogenic silver nanoparticles produced by Fusarium chlamydosporum and Penicillium chrysogenum at non-cytotoxic doses. Chemosphere 2019;218:477–86.
[57] Saratale RG, Benelli G, Kumar G, Kim DS, Saratale GD. Bio-fabrication of silver nanoparticles using the leaf extract of an ancient herbal medicine, dandelion (Taraxacum officinale), evaluation of their antioxidant, anticancer potential, and antimicrobial activity against phytopathogens. Environ Sci Pollut Res - Int 2018;25:10392–406.
[58] Manikandan V, Velmurugan P, Park J-H, Chang W-S, Park Y-J, Jayanthi P, et al. Green synthesis of silver oxide nanoparticles and its antibacterial activity against dental pathogens. Biotech 2017;7(72).
[59] Saravana Kumar P, Balachandran C, Duraipandiyan V, Ramasamy D, Ignacimuthu S, Al-Dhabi NA. Extracellular biosynthesis of silver nanoparticle using Streptomyces sp. 09 PBT 005 and its antibacterial and cytotoxic properties. Appl Nanosci 2015;5:169–80.
[60] Mukherjee P, Ahmad A, Mandal D, Senapati S, Sainkar SR, Khan MI, et al. Fungus-mediated synthesis of silver nanoparticles and their immobilization in the mycelial matrix: a novel biological approach to nanoparticle synthesis. Nano Lett 2001;1:515–9.
[61] Remya RR, Rajasree SRR, Aranganathan L, Suman TY. An investigation on cytotoxic effect of bioactive AgNPs synthesized using Cassia fistula flower extract on breast cancer cell MCF-7. Biotechnol Rep 2015;8:110–5.
[62] Park EJ, Bae E, Yi J, Kim Y, Choi K, Lee SH, et al. Repeated-dose toxicity and inflammatory responses in mice by oral administration of silver nanoparticles. Environ Toxicol Pharmacol 2010;30:162–8.
[63] Takenaka S, Karg E, Roth C, Schulz H, Ziesenis A, Heinzmann U, et al. Pulmonary and systemic distribution of inhaled ultrafine silver particles in rats. Environ Health Perspect 2001;109:547–51.
[64] Lee TY, Liu MS, Huang LJ, Lue SI, Lin LC, Kwan AL, et al. Bioenergetic failure correlates with autophagy and apoptosis in rat liver following silver nanoparticle intraperitoneal administration. Part Fibre Toxicol 2013;10(40).
[65] Kim YS, Kim JS, Cho HS, Rha DS, Kim JM, Park JD, et al. Twenty-eight-day oral toxicity, genotoxicity, and gender-related tissue distribution of silver nanoparticles in Sprague-Dawley rats. Inhal Toxicol 2008;20:575–83.
[66] Heydrnejad MS, Samani RJ, Aghaeivanda S. Toxic effects of silver nanoparticles on liver and some hematological parameters in male and female mice (Mus musculus). Biol Trace Elem Res 2015;165:153–8.
[67] Campagnolo L, Massimiani M, Vecchione L, Piccirilli D, Toschi N, Magrini A, et al. Silver nanoparticles inhaled during pregnancy reach and affect the placenta and the foetus. Nanotoxicology 2017;11:687–98.
[68] Johnston HJ, Hutchison G, Christensen FM, Peters S, Hankin S, Stone V. A review of the in vivo and in vitro toxicity of silver and gold particulates: particle attributes and biological mechanisms responsible for the observed toxicity. Crit Rev Toxicol 2010;40:328–46.
[69] Kteeba SM, El-Ghobashy AE, El-Adawi HI, El-Rayis OA, Sreevidya VS, Guo L, et al. Exposure to ZnO nanoparticles alters neuronal and vascular development in zebrafish: acute and transgenerational effects mitigated with dissolved organic matter. Environ Pollut 2018;242:433–48.
[70] Umezawa M, Onoda A, Korshunova I, ACØ J, Koponen IK, Jensen KA, et al. Maternal inhalation of carbon black nanoparticles induces neurodevelopmental changes in mouse offspring. Part Fibre Toxicol 2018;15(1):36.
[71] Onoda A, Takeda K, Umezawa M. Pretreatment with N-acetyl cysteine suppresses chronic reactive astrogliosis following maternal nanoparticle exposure during gestational period. Nanotoxicology 2017;11(8):1012–25.